Bistable-soliton pulse propagation: Stability aspects

R. H. Enns and S. S. Rangnekar
Department of Physics and Theoretical Science Institute, Simon Fraser University, Burnaby, British Columbia, Canada V5A 1S6

A. E. Kaplan
Department of Electrical and Computing Engineering, The Johns Hopkins University, Baltimore, Maryland 21218
(Received 10 March 1987)

Making use of numerical collision simulations, we have examined the stability of the bistable solitary-wave solutions (predicted earlier by Kaplan [Phys. Rev. Lett. **55**, 1291 (1985) and IEEE J. Quant. Electron. **QE-21**, 1538 (1985)]) to the generalized nonlinear Schrödinger equation for a wide range of nonlinear functions $f(I)$, I being the intensity. Gradations of stability have been observed, ranging from absolute instability through "weak" solitons to "robust" solitons. For all models studied, it was found that $dP/d\bar{\delta}<0$ guarantees unconditional instability while $dP/d\bar{\delta}>0$ is a necessary condition for the existence of weak and robust solitons. Here P is the energy of the solitary pulse and $\bar{\delta}$ is a propagation parameter. Sufficiency conditions for robustness of the soliton have also been suggested. We have further demonstrated that it is possible to construct physically realistic nonlinear models $f(I)$ for which robust bistable solitons exist.

I. INTRODUCTION

It has been recently demonstrated by Kaplan[1] that for a certain class of nonlinear functions $f(|E|^2)$, bistable (more generally, multistable) solitary-wave solutions to the generalized nonlinear Schrödinger equation

$$2i\partial E/\partial z+\partial^2 E/\partial x^2+Ef(|E|^2)=0 \tag{1}$$

can exist which carry the same energy P but have distinctly different profiles. Restricting ourselves to one-dimensional optical pulse propagation (the same equation applies to two-dimensional self-trapping[2]), E is the complex electric field amplitude; $z\propto z_1, z_1$ being the distance coordinate in the direction of propagation; while x is proportional to $t-z_1/v_g$, t being the time variable and v_g the group velocity. For the Kerr nonlinearity, $f(|E|^2)=a|E|^2$ ($a=$const), Eq. (1) is the well-known cubic nonlinear Schrödinger equation.[2-5] Multistable solitary-wave solutions do not occur for this nonlinearity. They may exist if either the nonlinear function $f(I)$, where $I\equiv|E|^2$ is the intensity, is changing its sign or is a steplike function. Possible higher-order nonlinear optical mechanisms leading to such $f(I)$ are multiphoton resonances and light-induced phase transitions (see, e.g., Ref. 1).

Because they may prove to be of considerable importance for such nonlinear optical applications as fiber optics communication with undistorted pulses,[4,5] compression of optical pulses,[4-6] and optical switching and bistability,[7] we shall examine in this paper in considerable detail the vital issue of the stability of these new bistable solitary-wave solutions. This stability issue was raised by the present authors in a recent paper,[8] the detailed arguments and additional numerical evidence being left for the present paper. It is well known that the nondegenerate solitary-wave solutions of the cubic nonlinear Schrödinger equation are stable against both small and large perturbations. In particular, two such solitary waves on colliding with each other survive their mutual strong nonlinear interaction and emerge after the collision with their profiles and velocities unchanged,[2] i.e., they are *solitons*. These solitons have been observed in optical fibers.[4]

Since the cubic nonlinear equation is by far the most well known of the nonlinear Schrödinger-like equations studied to date, the distinction between stability against small and large perturbations has never been clearly drawn in the literature. For such (and other)[9] nonlinear equations, the conditions of stability from small-perturbation analysis are often regarded as universal criteria for soliton existence. As shall be demonstrated, for highly nonlinear Schrödinger equations with their $f(I)$ differing substantially from the cubic nonlinearity, stability against small perturbations alone (as well as instability against large perturbations alone) does not provide a complete description of stability of solitary-wave solutions of highly nonlinear Schrödinger equations.

To explore the issue of the stability of bistable solitary waves we will proceed in this paper as follows. In Sec. II we introduce a variety of nonlinear models which exhibit bistability for certain ranges of the parameters. Two basic categories of models are considered, viz., polynomials models, particularly those in which the terms have opposite signs, and steplike models. For several of these models the solitary-wave solutions and corresponding energy formula are obtained either analytically or numerically. The stability of these solutions is investigated numerically in the next two sections by allowing two solitary pulses to collide. Collisions of a solitary pulse with nonsolitary wave profiles have also been considered. The explicit numerical scheme used in the collision studies is outlined in Sec. III, the results being presented in Sec. IV. To interpret our collision results,

we have introduced[8] the notion of "robust" solitons as distinct from "weak" solitons. The latter are stable against (sufficiently) small perturbations whereas the former ones are stable against any possible perturbations, including large perturbations in the form of collisions with other solitary waves (as well as with nonsoliton pulses). The solitons of the cubic nonlinear Schrödinger equation are robust in this sense. It is found that some models exhibit robust (in particular bistable robust) solitons while others display weak solitons. Still others have solitary solutions which are unstable against *any* (even extremely small) perturbations.

Based upon such models, we suggest in Sec. V a general stability criterion for arbitrary $f(I)$. For all models studied it was found that $dP/d\bar{\delta}>0$ guarantees stability against (sufficiently) small perturbations whereas $dP/d\bar{\delta}<0$ guarantees unconditional (absolute) instability. Here $\bar{\delta}$ is a parameter which correlates with the height and width of the solitary-wave solution (the larger the value of $\bar{\delta}$, the taller and narrower the solitary pulse). This condition was first proposed by Kaplan,[1] but without the collision results presented here, nothing could be said about its range of applicability. Further, although we find that $dP/d\bar{\delta}>0$ is a necessary condition, it is not sufficient to guarantee "robustness" of the soliton. Sufficiency conditions for robustness are suggested in Sec. V.

In addition to any possible practical applications, the findings presented here are important from a *conceptual* viewpoint because of their implications for other nonlinear evolution equations of physical interest which may display either multistability for appropriately chosen nonlinearities or the existence of both robust and weak solitons.

II. BISTABLE SOLITARY WAVES

Solitary-wave solutions of Eq. (1) of the form

$$E(x,z)=U(x-wz)\exp\left[\frac{i\delta z}{2}+iwx\right] \tag{2}$$

are sought with $U=|E|$ a real function satisfying the condition $U\to 0$ as $|y\equiv x-wz|\to\infty$, δ a real constant, and w playing the role of a velocity parameter. $w>0$ (<0) corresponds to solitary waves propagating with a velocity less (greater) than the group velocity. To have a collision between two solitary waves it is necessary to have $w\neq 0$ for at least one of the pulses.

On substituting (2) into Eq. (1), the following equation for U results:

$$\frac{d^2U}{dy^2}+U[f(U^2)-\bar{\delta}]=0 \tag{3}$$

with $\bar{\delta}\equiv\delta+w^2$. Subject to the condition that U (and its first derivative) $\to 0$ as $|y|\to\infty$, the first integral of (3) is of the form

$$(dU/dy)^2=2\int_0^U U[\bar{\delta}-f(U^2)]dU\ . \tag{4}$$

Equation (4) can only be integrated analytically for particularly simple forms of the nonlinear function $f(U^2)$. In general, one has to integrate (4) [or (3)] numerically (e.g., using a Runge-Kutta scheme) to determine the profile U. Specific examples of both situations shall be given shortly.

Once $U(y)$ has been determined, the energy associated with the solitary wave is given by $P=\int_{-\infty}^{\infty}|E|^2dy=\int_{-\infty}^{\infty}U^2dy$. One need not,[1] however, explicitly determine $U(y)$ to find P since it follows directly from (4) that

$$P(\bar{\delta})=\int_0^{I_m(\bar{\delta})}\frac{dI}{\sqrt{\bar{\delta}-F(I)}}\ , \tag{5}$$

where

$$F(I)=\frac{1}{I}\int_0^I f(I)dI,\quad F(0)=0 \tag{6}$$

and I_m is defined as the minimum positive root of the equation $F(I)=\bar{\delta}$. Physically, I_m is the peak intensity of the solitary wave. Multistability occurs when corresponding to a given value of P more than one value of the parameter $\bar{\delta}$ is possible.

We shall now consider some specific models for $f(|E|^2)$, the majority of which display multistability for certain ranges of the parameters.

A. Polynomial models

The physical basis of polynomial models rests on the fact that an n-photon process for a two-level system has a transition probability which varies as the nth power of the incident intensity. The polynomial models are made up of combinations of different n-photon processes, one-photon processes dominating at lower intensities, higher-order photon processes contributing at higher intensities. Which particular polynomial models correspond to experimental reality in a given material is beyond the scope of this paper.

To build a polynomial model with bistability present, first consider $f(I)=aI^n$ with both a and $n>0$. Making use of (5) and (6), one can *analytically* show that the energy $P\sim(\bar{\delta})^{1/n-1/2}$. For $n=1$ (cubic Schrödinger case), $dP/d\bar{\delta}>0$; for $n=2$, $dP/d\bar{\delta}=0$; for $n=3$, $dP/d\bar{\delta}<0$, and so on.

In order to demonstrate the *change* of stability behavior of solitary pulses as related to the behavior of $P(\bar{\delta})$, we have to consider nonlinear models formed from combinations of polynomial terms.

As the simplest example, we choose the polynomial model $f=a_1I+a_2I^2$, with a_1,a_2 either positive or negative, which was considered by Cowan, Enns, Rangnekar, and Sanghera.[10] For $a_1,a_2>0$, the energy curve P versus $\bar{\delta}$ should have a positive slope when the a_1I term dominates and flatten out (i.e., slope $\to 0$) when the second term becomes important. Actually, from (5) and (6) one finds *exactly* that for this case the normalized energy

$$\rho=P\sqrt{a_2/3}=\frac{\pi}{2}-\arcsin\left[\frac{1}{\sqrt{1+\beta}}\right]\ , \tag{7}$$

where

$$\beta\equiv\frac{16}{3}\frac{a_2}{a_1^2}\bar{\delta}\ .$$

The plot of Eq. (7) in Fig. 1(a) is in agreement with our qualitative argument. If one changes the signs, i.e., either

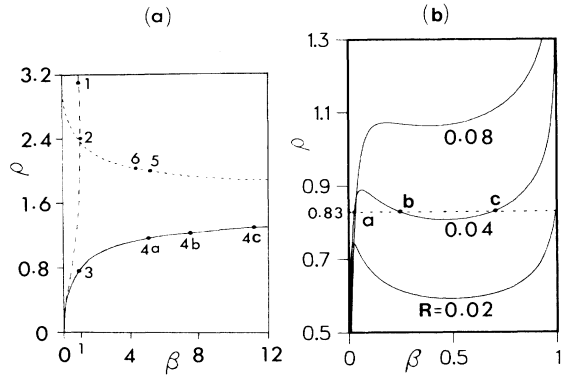

FIG. 1. Normalized energy ρ vs the parameter β for some polynomial models $f(I)$ discussed in the text; (a) Models corresponding to Eq. (7), ——; Eq. (8), — — —; Eq. (9), ----. Collision results for solitary-wave profiles corresponding to the points 1,2,3, . . . , 6 were presented in Cowan *et al.* (Ref. 10). The numbers correlate with the figure captions in that reference. The observed collision behavior was as follows: Quasisoliton (1,2,3); dispersive (4*a*,5), dispersive plus radiative spiking (4*b*), and explosive (4*c*,6). (b) Polynomial model defined by Eq. (10) for different R values.

(a) $f=a_1I-a_2I^2$, or (b) $f=-a_1I+a_2I^2$, with both a_1, $a_2>0$, analytic formulas for ρ may also be easily obtained, viz., for case (a)

$$\rho=\ln\left[\frac{\sqrt{1-\beta}}{1-\sqrt{\beta}}\right], \tag{8}$$

while for (b),

$$\rho=\frac{\pi}{2}+\arcsin\left[\frac{1}{\sqrt{1+\beta}}\right]. \tag{9}$$

Equations (8) and (9) are also plotted in Fig. 1(a). From the viewpoint of constructing a polynomial model with bistability present, one finds from these (and other) simple models that, except for the $n=2$ case which is special, a term of the structure aI^n in the polynomial with $n>0$ *but* $a<0$ will have a contribution to $dP/d\bar{\delta}$ of the *opposite* sign to the situation when $a>0$. This is seen, e.g., in Fig. 1(a), for the case $f=-a_1I+a_2I^2$. (It should be noted that if *both* coefficients of I and I^2 are negative, then there is no solitary-wave solution.)

Thus, e.g., the polynomial model $f=-a_1I+a_2I^2-a_3I^3$ with $a_1,a_2,a_3>0$ would yield a *U-shaped* $P(\bar{\delta})$ curve with two values of $\bar{\delta}$ possible for a given P above some critical value P_{cr}. On the other hand, for the polynomial model[1]

$$f=a_1I+a_2I^3-a_3I^5 \tag{10}$$

an *N-shaped* $P(\bar{\delta})$ curve would be expected to result by suitably adjusting a_1, a_2, and a_3 with each of the 3 branches of the N associated with one of the terms of $f(I)$. Thus for a certain range of these parameters, there would exist 3 values of $\bar{\delta}$ for a given value of P. Unfortunately, neither Eq. (5) for the energy P nor Eq. (4) for the solitary wave profile U can be solved analytically for a complex polynomial model such as that given by (10). For this particular model, we have numerically integrated Eq. (4) for different values of $\bar{\delta}$ using a standard fourth-order Runge-Kutta scheme. The area under the U^2 curve then gave us P as a function of $\bar{\delta}$. For a given value of the ratio $R=a_1a_3/a_2^2$, a universal energy curve results if $(a_1\sqrt{a_3/a_2}/a_1)^{1/2}P\equiv\rho$ is plotted against $(\sqrt{a_3/a_2}/a_1)(\bar{\delta}/\bar{\delta}_\infty)\equiv\beta$ where $\bar{\delta}_\infty$ is the value of $\bar{\delta}$ at which $d\rho/d\beta\to\infty$. Fig. 1(b) shows the $\rho(\beta)$ curves obtained for $R=0.02$, 0.04, and 0.08 for which $\bar{\delta}_\infty=4.75$, 2.62, and 1.55, respectively. Bistability occurs for $R\lesssim0.08$. That is, for, say, fixed values of a_1 and a_3, there is some minimum value of a_2 for which bistability is possible. This was to be expected from our earlier qualitative argument. Given the qualitative rule of thumb outlined above, clearly other polynomial models could be easily invented for which multistability is possible for certain ranges of the parameters. As with (10), the solitary-wave profiles and energy curves would have to generally be obtained numerically.

B. "Smooth" step-function models

Kaplan[1] has already noted that both the "sharp" step nonlinearity

$$f(I)=\begin{cases}0, & I<I_0\\ \Delta, & I>I_0\end{cases} \tag{11}$$

and the "smooth" step nonlinearity

$$f(I)=\begin{cases}0, & I\le I_0\\ \Delta\left[1-\dfrac{I_0^2}{I^2}\right], & I\ge I_0\end{cases} \tag{12}$$

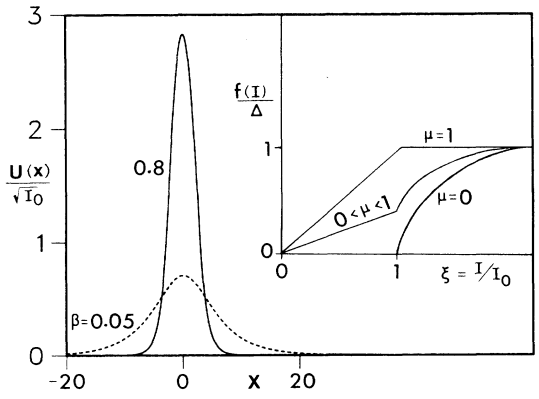

FIG. 2. Solitary-wave profiles $U(x)/\sqrt{I_0}$ for $\mu=0.2$, $\Delta=1$ and two representative β values calculated from Eqs. (18)–(20). Inset: Schematic representation of $f(I)$ for linear + smooth-step model, Eq. (16).

both with $\Delta>0$ can have more than one solitary-wave solution corresponding to the same value of P. From the viewpoint of numerically studying the "collision" of solitary waves propagating according to Eq. (1), smooth step-function models, i.e., those which do not have a discontinuity in $f(I)$, are more desirable to work with to avoid numerical difficulties due to the step function, particularly if the step is large. Furthermore, smooth steps are more realistic. For this reason, we shall confine our attention here to smooth step-function models. Equation (12), which is the simplest of such models, is sketched in the inset of Fig. 2 (the $\mu=0$ curve).

For this nonlinear model, Eq. (5) may be readily integrated yielding the normalized energy

$$\rho=P\Delta^{1/2}/I_0 = \{1/\beta^{1/2}+[\arccos(-\beta^{1/2})]/(1-\beta)^{1/2}\}/(1-\beta) \tag{13}$$

with $\beta\equiv\bar{\delta}/\Delta$. The inset of Fig. 3 corresponds to Eq. (13), there existing two branches for $\rho>\rho_{cr}\simeq 5.55$ [$\beta_{cr}=\beta(\rho_{cr})\simeq 0.15$]. From Eq. (4), the corresponding solitary-wave solution at $z=0$ is found to be

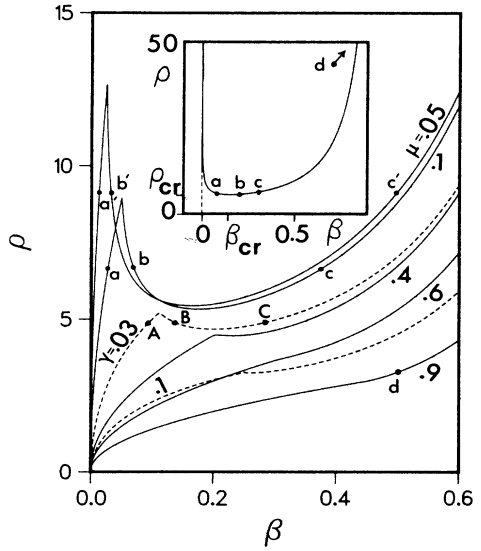

FIG. 3. Normalized energy ρ vs β for some smooth-step models defined in text: Solid curves: Eq. (17), linear + smooth step model for various μ values. Dashed curves: linear + quadratic + smooth-step model (21) for $\mu=0.1$ and different γ values. Inset: $\rho(\beta)$ given by Eq. (13) (smooth-step model) of text.

$$U(x)/I_0^{1/2}=\begin{cases}\exp[(\Delta\beta)^{1/2}(x_0-|x|)], & |x|\geq x_0\\ [(1+\beta^{1/2}\cos\{2[\Delta(1-\beta)]^{1/2}x\})/(1-\beta)]^{1/2}, & |x|\leq x_0\end{cases} \tag{14}$$

with

$$x_0=\arccos(-\beta^{1/2})/2[\Delta(1-\beta)]^{1/2}\,. \tag{15}$$

In Sec. IV, we shall find that robust solitons exist for $\beta>\beta_{cr}$ but not for $\beta<\beta_{cr}$. The question naturally arises whether one can have two robust solitons corresponding to the *same* energy for smooth step-function models. For this to occur, one needs, as for the polynomial model (10), an N-shaped (rather than U-shaped) $\rho(\beta)$ curve. As pointed out earlier for the Kerr nonlinearity $f(I)=\alpha I$, ($\alpha>0$), $dP/d\bar{\delta}>0$. Furthermore, this nonlinearity corresponds to the cubic case with known robust solitons. This suggests that we "splice" the linear $f(I)$ onto the smooth-step model creating the "linear + smooth-step" model, viz.,

$$f(I)=\begin{cases}\alpha I, & I\leq I_0\\ \Delta\left[1-(1-\mu)\dfrac{I_0^2}{I^2}\right], & I\geq I_0\end{cases} \tag{16}$$

with both $\alpha,\Delta>0$, $\mu=\alpha I_0/\Delta$, and $0<\mu<1$. Equation (16) is sketched in the inset of Fig. 2. For $\alpha=\mu=0$, it reduces to the "smooth-step" model (12), while for $\mu=1$ it corresponds to the "clipped" Kerr nonlinearity. Equations (4) and (5) may be analytically solved for the linear + smooth-step model yielding the normalized ($\rho\equiv P\Delta^{1/2}/I_0$) energy formula

$$\rho(\beta)=\begin{cases}2[\beta^{1/2}+(\beta-\beta_{cr_1})^{1/2}]^{-1}+[(\beta-\beta_{cr_1})^{1/2}+2\Delta^{1/2}(1-\frac{3}{2}\beta_{cr_1})x_0]/(1-\beta) & \text{for } \beta\geq\beta_{cr_1}=\mu/2\\ 2\beta^{1/2}/\beta_{cr_1} & \text{for } \beta\leq\beta_{cr_1}\end{cases} \tag{17}$$

and solitary-wave profiles

$$U(x)/I_0^{1/2}=\begin{cases}\beta^{1/2}\{\beta^{1/2}\cosh[(\Delta\beta)^{1/2}(x\mp x_0)]\pm(\beta-\beta_{cr_1})^{1/2}\sinh[(\Delta\beta)^{1/2}(x\mp x_0)]\}^{-1} & \text{for } x\begin{cases}\geq x_0\\ \leq -x_0\end{cases}\\ (\{(1-\frac{3}{2}\beta_{cr_1})+[(1-\frac{3}{2}\beta_{cr_1})^2-(1-2\beta_{cr_1})(1-\beta)]^{1/2}\cos[2\sqrt{\Delta(1-\beta)}x]\}/(1-\beta))^{1/2} & \text{for } |x|\leq x_0,\ \beta>\beta_{cr_1}\end{cases} \tag{18}$$

and

$$U(x)/I_0^{1/2}=\left[\frac{\beta}{\beta_{cr_1}}\right]^{1/2}\operatorname{sech}[(\Delta\beta)^{1/2}x] \quad \text{for } \beta<\beta_{cr_1} \tag{19}$$

with

$$x_0\equiv\arccos\left[\frac{(-\beta+\frac{3}{2}\beta_{cr_1})}{[(1-\frac{3}{2}\beta_{cr_1})^2-(1-2\beta_{cr_1})(1-\beta)]^{1/2}}\right]\Big/2\sqrt{\Delta(1-\beta)}\ . \tag{20}$$

For $\alpha=0$, $\beta_{cr_1}=0$ and these formulas reduce to those for the smooth-step model. Solitary-wave profiles $U(x)/I_0^{1/2}$ calculated from (18)–(20) are shown in Fig. 2 for $\mu=0.2$, $\Delta=1$ and two representative β values. The larger the value of β the taller and narrower is the solitary pulse. The solid curves in Fig. 3 illustrate the behavior of $\rho(\beta)$ given by (17) as a function of μ. For $\mu\lesssim 0.42$, the $\rho(\beta)$ curve has *three* branches, a lower positive-slope branch for $\beta<\beta_{cr_1}$, an upper positive-slope branch for $\beta>\beta_{cr_2}$ (corresponding to the minimum of the "dip"), and a negative-slope branch for $\beta_{cr_1}<\beta<\beta_{cr_2}$. Since $\mu=\alpha I_0/\Delta$, the existence of a threshold value (i.e., approximately 0.42) for μ tells us that for given values of α and I_0 there is a minimum value of the "step size" Δ required for two positive-slope branches to occur.

It is clear from our discussion of polynomial models that *analytic* formulas for both $\rho(\beta)$ and $U(x)$ are also obtainable for the "linear + quadratic + smooth-step" model

$$f(I)=\begin{cases} a_1I+a_2I^2, & I\le I_0 \\ \Delta\left[1-(1-\mu-6\gamma)\dfrac{I_0^2}{I^2}\right], & I\ge I_0 \end{cases} \tag{21}$$

with $a_1,a_2,\Delta>0$ and $\mu=a_1I_0/\Delta$, $\gamma=a_2I_0^2/6\Delta$. We shall not write the lengthy formulas here. The dashed lines in Fig. 3 show the effect on $\rho(\beta)$ of increasing γ for a given μ value ($\mu=0.1$). As γ is increased from zero, the negative-slope region between $\beta_{cr_1}=\frac{1}{2}\mu+2\gamma$ and β_{cr_2} shrinks and eventually disappears. Multivaluedness is lost.

The linear + smooth-step model and its sequel (21) were artificially created by splicing and also displayed a somewhat unrealistic discontinuity in slope. More physically realistic smooth step-function models displaying bistability may be created which do not involve these features, e.g.,

$$f(I)/\Delta=\frac{\mu\xi+\xi^n}{1+\mu\xi+\xi^n} \tag{22a}$$

with $\xi=I/I_0$ and n a positive integer. Equation (22a) is plotted in Fig. 4 for $n=5$ and some representative μ values. From our discussion of the polynomial models, it is clear that (22a) will yield an N-shaped energy curve for $n\ge 3$ and μ less than some critical value, the value of μ_{cr} depending on n. For $\mu=0$ and $n\to\infty$, this model approaches the step nonlinearity (11). The nonlinear function (22a) corresponds physically to *combined* one-photon and n-photon resonances with a resonant saturation.

Another model displaying bistability for $n\ge 3$ is the following

$$f(I)/\Delta=\mu\xi+\frac{\xi^n}{1+\xi^n}\ , \tag{22b}$$

which is sketched in the inset of Fig. 4, also for $n=5$. Equation (22b) corresponds to a Kerr nonlinearity plus a saturable n-photon resonance. Note that unlike model (22a), $f(I)$ given by (22b) does not saturate at large I but becomes Kerr-like once again. Still other more complex models have been created and studied.

For both models (22a) and (22b), Eq. (3) has been solved for U using a standard Runge-Kutta scheme and then the $\rho\equiv P\sqrt{\Delta}/I_0$ versus $\beta\equiv\bar{\delta}/\Delta$ curves obtained for different n values. Figure 5 shows typical energy curves (the solid curves) for $n=5$ for model (22a), bistability occurring for $\mu\lesssim 0.36$. The critical value of μ increases with increasing n, e.g., $\mu_{cr}\simeq 0.13$ for $n=3$ and (approximately) 0.9 for $n=10$. Note that the cusp which occurred at β_{cr_1} in Fig. 2 originating from the discontinuity in slope in the nonlinear function $f(I)$, has now been rounded off. Also shown (dashed lines) in Fig. 5 are the energy curves for model (22b) with $n=5$. In this case

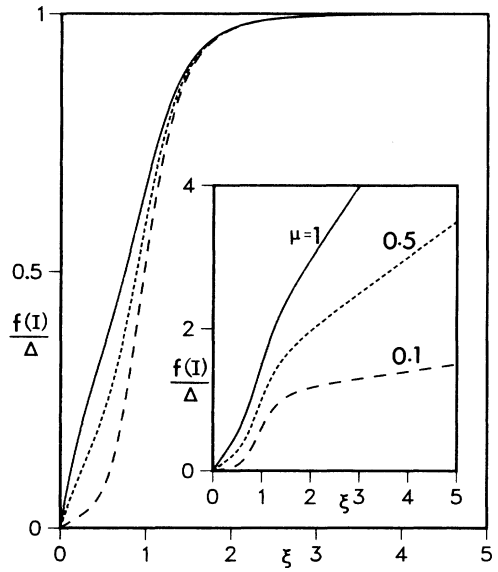

FIG. 4. Steplike model (22a) for $n=5$ and $\mu=0.1$, — — —; $\mu=0.5$; ----, $\mu=1$, ——. Inset: Steplike model (22b) for $n=5$ and $\mu=0.1$, — — —; $\mu=0.5$, ----; $\mu=1$, ——.

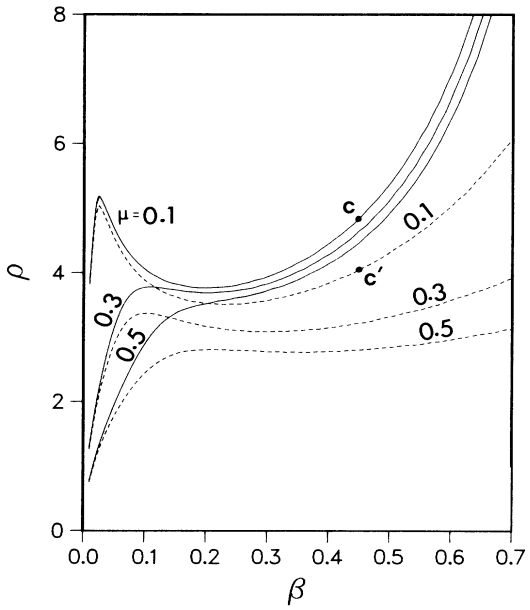

FIG. 5. Normalized energy ρ vs β for model (22a) (solid curves) and model (22b) (dashed curves) for $n=5$ and various μ values.

$\mu_{cr}\simeq 0.5$. For a given n value, μ_{cr} is larger for model (22b) than for (22a).

To study the stability of colliding solitary waves corresponding to the various points indicated schematically in Figs. 1, 3, and 5, we next introduce a simple numerical scheme to simulate Eq. (1).

III. NUMERICAL SCHEME FOR COLLISION STUDIES

To study the collision process, Eq. (1) was simulated numerically, an explicit three-step scheme being employed, the central difference approximation (CDA), being used for $\partial E/\partial z$ on all z steps except the first. That is, separating E into real and imaginary parts, viz., $E=u+iv$, labeling the mesh points (x,z) by m,n and setting $\Delta z\equiv k$, $\Delta x\equiv h$, Eq. (1) was replaced by the coupled system

$$u_{m,n+1}=u_{m,n-1}-(k/h^2)[v_{m+1,n}-2v_{m,n}+v_{m-1,n}]-k(vf)_{m,n} \tag{23}$$

$$v_{m,n+1}=v_{m,n-1}+(k/h^2)[u_{m+1,n}-2u_{m,n}+u_{m-1,n}]+k(uf)_{m,n} \tag{24}$$

with $k/h^2\ll 1$ in our numerical runs. [It was found that the computation time was shorter when working with the coupled real equations than trying to solve the complex equation (1) directly.] To obtain accurate values of u,v for the first step to use in this three-step scheme, the first step Δz was further subdivided into several hundred smaller steps and a forward difference approximation (FDA), e.g., $(\partial u/\partial z)=(u_{n+1}-u_n)/k$, used. The FDA, which is less accurate for a given step size k than the CDA, could not be used for large z because then numerical instabilities were observed to occur.

To keep the x range (and thus the computing time) down, periodic boundary conditions were imposed by taking the extreme right and left mesh points to be adjacent in the approximation to E_{xx} in (23) and (24). As a consequence, pulses impinging on the boundaries reappear on opposite edges. Care was also taken to work with input pulses whose widths were *narrow* compared to the grid width in the x direction and to the initial separation of the pulses.

To monitor the accuracy of our numerical runs as well as to guide us in choosing an optimal mesh size, we derived the first three invariants (i.e., quantities independent of z) of Eq. (1) for arbitrary $f(I)$, viz.,

$$J_1\equiv P=\int_{-\infty}^{\infty} I\,dx\ , \tag{25}$$

$$J_2=i\int_{-\infty}^{\infty}(EE_x^*-\text{c.c.})dx\ , \tag{26}$$

$$J_3=\int_{-\infty}^{\infty}\left[|E_x|^2-\int_0^I f(s)ds\right]dx\ . \tag{27}$$

These invariant quantities are consistent with the first three conservation laws[2] for the particular case of the cubic nonlinear Schrödinger equation. For our input pulses, initially $J_2=0$. We found it convenient to monitor the maximum value of $|\Delta J_1/J_1|$ and $|\Delta J_3/J_3|$. In all our computer runs, $\max|\Delta J_1/J_1|$ was better (usually very much better) than 1.5% and $\max|\Delta J_3/J_3|$ better than about 5%. The latter tended to be higher because of the derivative (E_x) term and the highly nonlinear function $f(s)$ in J_3.

In presenting our collision results in Sec. IV, we have chosen to plot $|E|$ which is a physically measurable quantity.

IV. COLLISION RESULTS

Kaplan's original proposed stability criterion[1] was that those solitary-wave profiles for which $dP/d\bar{\delta}$ (or $d\rho/d\beta$) >0 would be stable while those for which $dP/d\bar{\delta}<0$ would be unstable. This conjecture was based upon a small perturbation analysis of the step-function model (11).

Making use of the models introduced in Sec. II, this conjecture has been tested by allowing two solitary waves to collide with each other as well as with non-solitary-wave pulses. Large as well as small perturbations may be studied by this procedure. Although a wide variety of relative speeds were considered, in all the figures presented here [except for Fig. 7(a)] we have taken $w_L=-w_R=5$, where L and R refer to the pulses initially ($z=0$) on the left and right.

Since it was the first bistable model to be studied for solitary pulse collisions,[11] let us start with the smooth-step-function model (12). Keeping in mind that for this model $d\rho/d\beta>0$ for $\beta>\beta_{cr}\simeq 0.15$ and vice versa, consider the numerical runs illustrated in Fig. 6. We have selected input solitary-wave pulses calculated from (14) corresponding to the β values labeled a ($\beta_a=0.1$) and b ($\beta_b=0.2$) in the inset of Fig. 3. Figure 6(a) shows that in an a-a collision, the two pulses disperse after the interaction. On the other hand, in a b-b collision [Fig. 6(b)], the two pulses are solitonlike emerging from the collision un-

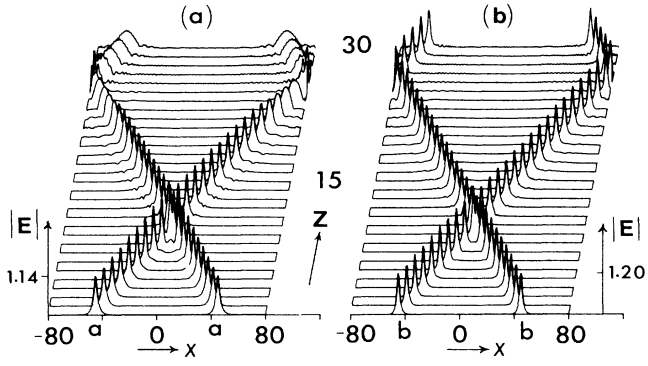

FIG. 6. Typical collision results for the smooth-step model (12). (a) For two solitary waves corresponding to point a in the inset of Fig. 3. (b) For two solitary waves corresponding to point b in the inset of Fig. 3. Parameters: $I_0=0.9$ for (a), 0.8 for b; $\Delta=3$. Mesh size: $\Delta x=0.08$, $\Delta z=0.003$.

changed. A "mixed" collision between pulses corresponding to points (a) and (c) of the inset was shown in Ref. 11, pulses (a) again dispersing, whereas pulse (c) was solitonlike in behavior. Still larger β values have been considered (e.g., a d-d collision (not shown here), where point d in the inset corresponds to $\beta=0.9$), *all* numerical runs being consistent with Kaplan's conjectured stability criterion. That is, those pulses for which $\beta>0.15$ are stable and survive the collision process unchanged and vice-versa.

On the other hand, Kaplan's stability criterion is *not* consistent with the strong solitary pulse collisions studied earlier by Cowan *et al.*[10] summarized schematically in Fig. 1(a). The points labeled 1,2,... refer to figure numbers (numerical runs) in Ref. 10. For both the models $f=a_1I+a_2I^2$ and $f=a_1I-a_2I^2$ (with $a_1,a_2>0$), $d\rho/d\beta>0$ for all β (no bistability present). Even though $d\rho/d\beta>0$, it was found that the solitary waves were not solitonlike in the collision process. For example, so-called "quasisoliton" behavior was observed for collisions of identical solitary pulses corresponding to points 1,2,3 in Fig. 1(a). That is, *smaller* solitonlike pulses emerged after the collision with velocities *differing* from those of the input pulses, the difference in energy being shed as radiation. For other values of β [see figure caption 1(a)], radiative or explosive behavior was observed. The question arises, why does Kaplan's criterion work for one model and not the other? An important clue was provided by the observation that solitary pulses corresponding to the various points in Fig. 1(a) *with* $d\rho/d\beta>0$ could survive collisions with *sufficiently small* (solitary *and* non-solitary) pulses. A nice example of this is illustrated in Fig. 7(a). The solitary pulse initially on the left corresponds to the point labeled 4a in Fig. 1(a). The pulse initially on the right is a *non-solitary-wave* profile obtained by multiplying the input solitary-wave pulse profile on the left by $\frac{1}{2}$. Because it is not a solitary wave, the pulse on the right begins to spread even before the collision. Nevertheless the solitary pulse experiences a sizable perturbation. Even though the solitary pulse cannot survive a collision with another identical pulse (it disperses), it survives the weaker collision in Fig. 7(a) apparently unchanged. Therefore the solitary pulse is "weakly" stable.

Let's now return to our study of bistable models. As pointed out by Kaplan,[12] a natural followup to the numerical study of the smooth step model would be to study the collision of two bistable solitary waves (which carry the same energy) in a medium with a nonlinearity such that for *both* of them $dP/d\delta>0$. Instead of a "U-shaped" energy curve, an "N-shaped" energy curve is required. In Sec. II, we have constructed several $f(I)$ which have this feature.

Let us first consider the polynomial model (10), the normalized energy curves having been shown in Fig. 1(b). Taking the $R=0.04$ curve, consider the three points labeled a ($\beta_a=0.027$), b ($\beta_b=0.218$), and c ($\beta_c=0.724$) *all* corresponding to the *same* $\rho(\simeq 0.83)$. For pulses a and c, $d\rho/d\beta>0$. An a-c collision was shown in Fig. 2 of Ref. 8, pulse a remaining unchanged after the collision but pulse c dispersing. This latter behavior is also illustrated in Fig. 7(b) where a b-c collision occurs. Both pulses flatten out after the collision, the behavior being expected for b (for which $d\rho/d\beta<0$) but not for c. By considering other β values on the upper positive-slope branch as well as other R values, we were forced to the general conclusion that solitary pulses belonging to the upper positive-slope branch are *not* stable against large perturbations (in the form of collisions with other pulses) even though $d\rho/d\beta>0$. We did find, however, that pulses on the upper positive-slope branch were stable against sufficiently small perturbations (see Fig. 1, Ref. 8), i.e., they are also "weakly" stable. On the other hand, pulses corresponding to $d\rho/d\beta<0$ were found to be unstable no matter how small the perturbation was (see, e.g., Fig. 3, Ref. 8). To distinguish between the stability displayed by

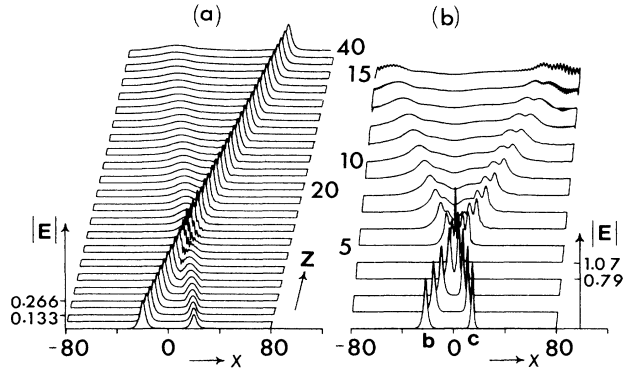

FIG. 7. (a) Stability of solitary wave (initially on left) corresponding to point 4a in Fig. 1(a) against collision with a non-solitary wave (initially on the right). Parameters: For pulse on left $a_1=4$, $a_2=61.8$, $\bar{\delta}=0.25$. $|w|=1.6$. Mesh size: $\Delta x=0.08$, $\Delta z=0.003$. (b) Collision result for polynomial model (10) for pulses corresponding to points b and c in Fig. 1(b). Parameters: $\bar{\delta}_b=0.452$, $\bar{\delta}_c=1.5$. Mesh size: $\Delta x=0.04$, $\Delta z=5\times10^{-4}$.

the solitary pulses, we have introduced the concept of weak solitons and robust solitons.[8] The latter are stable against large perturbations, in particular collisions with other large solitary waves. The solitary pulses on the upper positive slope of the smooth-step model and the lower positive slope branch of the polynomial model (10) are examples of robust solitons. Pulses corresponding to the upper positive-slope branch of the polynomial model and the two positive-slope curves in Fig. 1(a) are examples of weak solitons.

The condition $dP/d\bar{\delta}>0$ guarantees stability against (sufficiently) small perturbations, i.e., guarantees the existence of weak solitons. It is a necessary but not sufficient condition for robustness of a soliton. On the other hand, $dP/d\bar{\delta}<0$ guarantees unconditional instability. That $dP/d\bar{\delta}<0$ is associated with unconditional instability helps us to understand the results corresponding to the model $f=-a_1I+a_2I^2$ [Fig. 1(a)]. For this model, the slightest disturbance was observed to destroy the input solitary pulses.

Although we have shed considerable light on the stability issue, two important questions remain, viz.: Can two (or more) robust solitons corresponding to the same energy coexist? If so, what are the additional conditions (in addition to the necessary condition $dP/d\bar{\delta}>0$) on $f(I)$ to ensure robustness?

To answer the first question we next turn to the linear + smooth-step model (16). Referring to Fig. 3, we again select three points a ($\beta_a=0.031$), b ($\beta_b=0.065$), c ($\beta_c=0.4$) on the $\mu=0.1$ curve all corresponding to $\rho\simeq 6.97$. Figs. 8(a) and 8(b) show respectively an a-b and a b-c collision. It is clear that now *both* pulses a and c are robust solitons, whereas pulse b is unstable. Runs corresponding to other β and μ values, e.g., the points a',b',c' ($\rho\simeq 9.17$, $\beta_{a'}=0.013$, $\beta_{b'}=0.032$, $\beta_{c'}=0.5$) on the $\mu=0.05$ curve, confirm this behavior. Figure 9(a) shows a mixed a'-c' collision, both pulses behaving like "robust solitons." Robustness for $d\rho/d\beta>0$ occurs even when $\mu>\mu_{cr}$, i.e., even when multivaluedness is lost. Figure 9(b) illustrates a d-d collision where d corresponds to the point ($\beta_d=0.5$) indicated on the $\mu=0.9$ curve of Fig. 3. Consistent with our previous remarks, a pulse corresponding to point b' was found to be unstable against the slightest perturbation (see Fig. 3, Ref. 8).

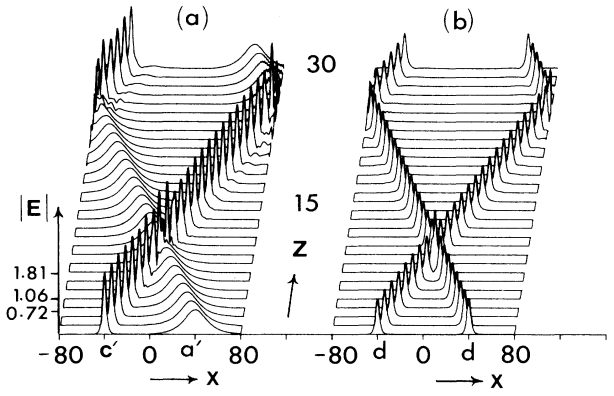

FIG. 9. Typical collision results for linear + smooth-step model (16). (a) For solitary waves corresponding to points a' and c' in Fig. 3. (b) For two solitary waves corresponding to points d on $\mu=0.9$ curve in Fig. 3.

One could argue that by constructing the linear + smooth-step model, we have perhaps guaranteed the existence of robust bistable solitons but that this model is very artificial. Can one construct other, perhaps more physically realistic, models displaying the same behavior? Our first attempt to answer this question was to modify the linear + smooth-step model, thus the introduction of the "linear + quadratic + smooth-step" model. Referring to the (dashed) $\gamma=0.03$ curve in Fig. 3, we considered three β values again labeled A ($\beta_A=0.095$), B ($\beta_B=0.134$), C ($\beta_C=0.288$) all corresponding to $\rho\simeq 4.91$. Figure 10 shows that the robust behavior persists for this model for pulses corresponding to

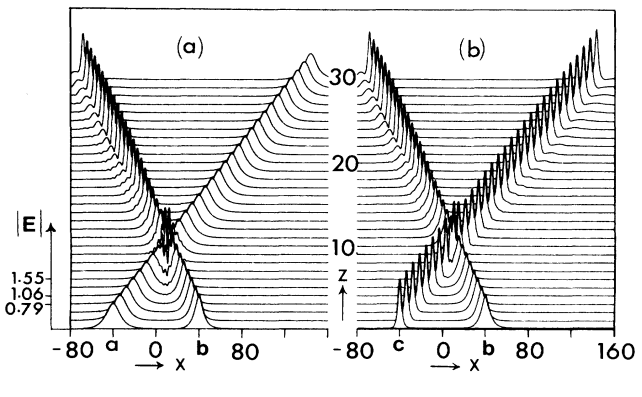

FIG. 8. Typical collision results for linear + smooth-step model (16). (a) For solitary waves corresponding to points a and b in Fig. 3. (b) For solitary waves corresponding to points c and b in Fig. 3. Parameters for Figs. 8–11: $\Delta=I_0=1$. Mesh size for Figs. 8–11: $\Delta x=0.08$, $\Delta z=3\times 10^{-3}$.

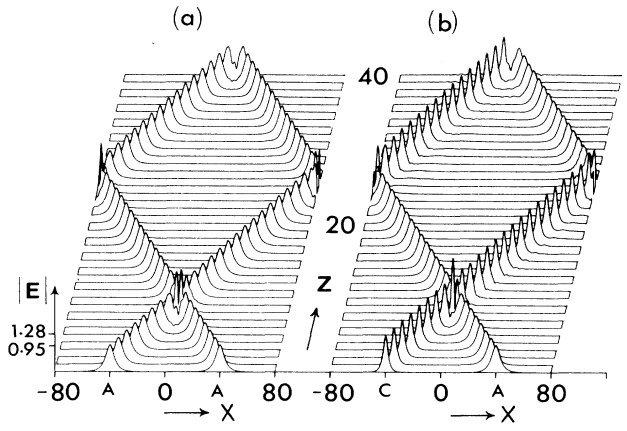

FIG. 10. Typical collision result for linear + quadratic + smooth-step model (21). (a) For two solitary waves corresponding to point A in Fig. 3. (b) For solitary waves corresponding to points A and C in Fig. 3.

$d\rho/d\beta > 0$. Pulses A and C are still solitonlike in the collision processes shown.

Both of the smooth-step models considered here involve splicing and are characterized by a discontinuity in the slope of $f(I)$. The two models defined by (22a) and (22b) have neither of these features, yet also display robust bistable soliton behavior for $d\rho/d\beta > 0$. Figure 11(a) shows, e.g., a collision between two pulses corresponding to the point c ($\beta_c = 0.45$) on the upper positive-slope branch of the solid $\mu = 0.1$ curve of Fig. 5. The pulses remain solitonlike even after a (somewhat artificial) second collision. Very similar behavior was also observed for the model defined by (22b), see Fig. 11(b) illustrating a c'-c' collision where c' ($\beta_{c'} = 0.45$) is the point indicated on the dashed $\mu = 0.1$ curve of Fig. 5.

Based on the models reported here and others that we have investigated, two additional conditions on $f(I)$ for robustness have been proposed[8] which are physically reasonable and consistent with all of the models that we have studied to date, viz., (i) $f(I)/I^2 = o(1)$ as $I \to \infty$, stability against collapse ("self-focusing"). (ii) $f(I)$ is a nonnegative and nondecreasing function for $I > 0$, stability against dispersion. Condition (i) prevents the occurrence of self-focusing singularities, which occur[13] for $f \sim aI^n$ ($a > 0$) for large I for $n \geq 2$. It excludes, e.g., the model $f = a_1 I + a_2 I^2 (a_1, a_2 > 0)$. Condition (ii) is introduced to rule out, e.g., the polynomial model (10) and the model $f = a_1 I - a_2 I^2$. If $f(I)$ decreases sufficiently at large I, then the derivative terms in Eq. (1) will predominate and it is well known that these terms tend to disperse or spread pulses.

In terms of a single multiphoton process dominating at large I so that $f \sim I^n$ (n an integer value) in this regime, the two additional conditions above define a "window" on $f(I)$ inside which there are only *two* possibilities for n, viz., $n = 0$ (corresponding to saturation) and $n = 1$ (becoming Kerr-like for large I). Models (22a) and (22b), for which robust bistable solitons have been shown to exist, illustrate these two cases.

In terms of stimulating the search for appropriate physical mechanisms, the conclusions just reached provide working guidelines to the type of nonlinearities needed to produce robust bistable solitons. Robust bistable solitons will occur if the $f(I)$ is Kerr-like at small I, has a sufficiently steep (equivalent to a three-photon, or higher order, process) jump at intermediate I and becomes flat or increases linearly at large I.

V. GENERAL CONCLUSIONS

From our collision results in Sec. IV we can draw the following general conclusions:

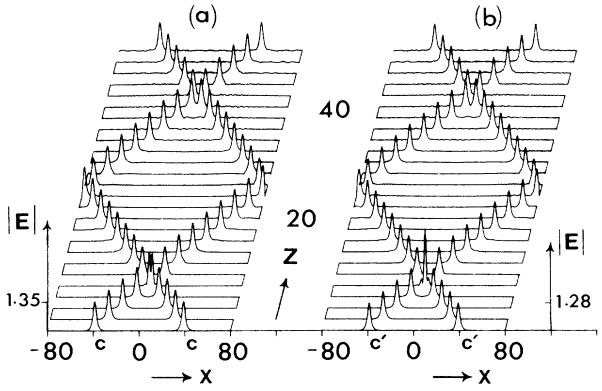

FIG. 11. Robust behavior of two solitary waves (a) corresponding to point c in Fig. 5(b), corresponding to point c' in Fig. 5.

(1) It is not sufficient in describing the solitary-wave solutions of the highly nonlinear Schrödinger equation to simply say that the solitary waves are stable or unstable. Our results demonstrate that there are *gradations* of stability. By introducing the concepts of weak and robust solitons, we have seen behavior ranging from absolute instability through weak solitons to robust solitons. This distinction has not been clearly made, if at all, in the existing literature. It also follows that the standard perturbation analysis of stability only distinguishes between weak solitons and absolutely unstable solitary waves, saying nothing about robustness.

(2) We have demonstrated that it is possible to construct physically realistic nonlinear models $f(I)$ for the generalized nonlinear Schrödinger equation for which *robust bistable solitons exist.* This is further confirmed by the recent numerical simulations of Enns and Rangnekar[14,15] on optical switching.

(3) We have refined Kaplan's original conjecture on stability, viz., $dP/d\bar{\delta} < 0$ guarantees unconditional instability, $dP/d\bar{\delta} > 0$ is a necessary condition for the existence of weak and robust solitons. It is not a sufficient condition for robustness. Some physically reasonable additional conditions have been suggested in Sec. IV.

ACKNOWLEDGMENTS

The work of A.E.K. is supported by the Air Force Office of Scientific Research. R.H.E. and S.S.R. acknowledge a grant from the Natural Sciences and Engineering Research Council of Canada.

[1](a) A. E. Kaplan, Phys. Rev. Lett. **55**, 1291 (1985); (b) IEEE J. Quantum Eectron. **QE-21**, 1538 (1985).

[2]V. E. Zakharov and A. B. Shabat, Zh. Eksp. Teor. Fiz. **61**, 118 (1971) [Sov. Phys.—JETP **34**, 62 (1972)].

[3]P. L. Kelley, Phys. Rev. Lett. **15**, 1005 (1965); R. Y. Chiao, E. Garmine, and C. H. Townes, *ibid.* **13**, 479 (1964); J. Satsuma and N. Yajima, Suppl. Prog. Theor. Phys. **55**, 284 (1974).

[4]L. F. Mollenauer, R. H. Stolen, and J. P. Gordon, Phys. Rev. Lett. **45**, 1095 (1980).

[5]H. Nakatsuka, D. Grishkowsky, and A. C. Balant, Phys. Rev.

Lett. **47**, 910 (1981); A. Hasegawa and Y. Kodama, Proc. IEEE **69**, 1145 (1981); A. Hasegawa and F. Tappert, Appl. Phys. Lett. **23**, 142 (1973); A. Hasegawa and Y. Kodama, Opt. Lett. **7**, 285 (1982); Y. Kodama and A. Hasegawa, *ibid.* **7**, 339 (1982).

[6]D. Grishkowky and A. C. Balant, Appl. Phys. Lett. **41**, 1 (1982); C. V. Skank, R. L. Fork, R. Yen, R. H. Stolen, and W. J. Tomlinson, *ibid.* **40**, 761 (1982).

[7]H. M. Gibbs, *Optical Bistability* (Academic, New York, 1985).

[8]R. H. Enns, S. S. Rangnekar, and A. E. Kaplan, Phys. Rev. A **35**, 466 (1987).

[9]S. Puri, Phys. Lett. **105A**, 443 (1984); S. E. Burkov and A. E. Lifshitz, *ibid.* **106A**, 71 (1984); D. Anderson, A. Bendenson, and M. Lisak, J. Plasma Phys. **21**, 259 (1970); M. I. Weinstain, SIAM J. Math. Annu. **16**, 472 (1985); T. B. Benjamin, Proc. R. Soc. London Ser. A **328**, 153 (1972); J. Bona, *ibid.* **344**, 363 (1975).

[10]S. Cowan, R. H. Enns, S. S. Rangnekar, and S. S. Sanghera, Can. J. Phys. **64**, 311 (1986).

[11]R. H. Enns and S. S. Rangnekar, Phys. Rev. Lett. **57**, 778 (1986).

[12]A. E. Kaplan, Phys. Rev. Lett. **57**, 779 (1986).

[13]Y. Kodama and M. J. Ablowitz, Stud. Appl. Math. **64**, 225 (1981).

[14]R. H. Enns and S. S. Rangnekar, Optics Lett. **12**, 108 (1987).

[15]R. H. Enns and S. S. Rangnekar, IEEE J. Quantum Electron. (to be published).